Critical Current Peaks at $3B_\Phi$ in Superconductors with Columnar Defects: Recrystallizing the Interstitial Glass

M. E. Gallamore, G. E. D. McCormack, and T. P. Devereaux
Department of Physics, University of Waterloo, Waterloo, Ontario Canada N2L 3G1
(Received 7 December 2003; published 5 August 2004)

The role of commensurability and the interplay of correlated disorder and interactions on vortex dynamics in the presence of columnar pins is studied via molecular dynamics simulations. Simulations of dynamics reveal substantial caging effects and a nonmonotonic dependence of the critical current with enhancements near integer values of the matching field B_ϕ and $3B_\phi$ in agreement with experiments on the cuprates. We find qualitative differences in the phase diagram for small and large values of the matching field.

DOI: 10.1103/PhysRevLett.93.067002 PACS numbers: 74.25.Qt, 67.40.Yv, 75.40.Mg

The rich phases of vortex matter in high temperature superconductors result from a complex interplay between disorder, interactions and fluctuations [1]. Of particular interest is the role of columnar defects created by heavy ion radiation in forming more effectively pinned phases of interacting vortices. Extended or correlated disorder is much more effective at pinning vortices than uncorrelated (pointlike) disorder and produces upward shifts of several tesla in the irreversibility lines and concomitantly larger critical currents.

The physics of 3D vortex pinning via correlated disorder can be approximately mapped onto the problem of interacting quantum bosons in the presence of uncorrelated disorder in 2D [2]. This has formed the basis for computational studies via quantum Monte Carlo simulations of local repulsive bosons [3] and exact diagonalization [4]. Several pinned phases of vortex matter emerge as a function of B/B_Φ, where B_Φ is the equivalent matching field where the number of vortices equals the number of defects. For the case where the pins outnumber the vortices ($B < B_\Phi$), a Bose-glass phase is formed where vortices are localized onto columnar defects and possess an infinite tilt modulus for tilts away from columnar alignment. For equal numbers of vortices and defects ($B = B_\Phi$), an analog to a Mott insulating phase exists which possesses an infinite compression modulus [2]. The existence of the Bose-glass phase is well documented [1,3], and evidence for the Mott phase has been found in recent magnetization relaxation measurements at low temperatures [5,6]. For the case when the vortices outnumber the pins ($B > B_\Phi$) the situation is much less clear. Recent work has suggested that vortices not accommodated to the columnar defects are caged by pinned vortices to form a weakly pinned "interstitial Bose" glass [2,7,8]. It has been conjectured that the melting temperature T_m decreases rapidly as the density of interstitial vortices increases for large fields, and either extends smoothly into the Bose glass phase [2] or shows a change in slope (kink) at $B = B_\Phi$ [7,8]. Some experiments [9–12] do not show substantial changes of the irreversibility line at B_Φ, while others show only a mild kink at B_Φ [5,6,13–15]. The change is even less significant for larger defect concentrations (larger B_Φ).

In analogy with the presence of Mott lobes in the dual superconducting-insulator transition in 3D, one would expect different phases at commensurate values of vortex filling for $B > B_\phi$. Nowak *et al.* found that the critical current in $Tl_2Ba_2CuO_{6+\delta}$ decreases for $B > B_\phi$ but then increases and goes through a maximum near $3B_\phi$ [6], which is currently unaddressed by theory.

One of the weakness of previous numerical studies [3,4] is the use of a short-range screened interaction which misses the softening of the shear modulus in the absence of pins in the weak field limit as noted by Fetter, Hohenberg and Pincus [2,16,17]. The purpose of this paper is to address the importance of this omission via 3D molecular dynamics (MD) simulations of vortices interacting via a long-range potential in the presence of columnar defects. Our key result is that the softening of the shear modulus in the low field limit has important implications for the phase diagram. We confirm the existence of a weakly pinned interstitial glass which becomes more weakly pinned as the field increases in agreement with previous studies of short-range interactions [4]. However we find a qualitatively new phase diagram for low fields where the interstitial glass melts near $B = B_\phi$ and recrystallizes at higher fields when the matching field is below a critical value. In this regime we find strong numerical evidence for enhanced values of the critical current near 3 times the matching field. This questions the quantitative appropriateness of the mapping of vortex physics onto the physics of the superconductor-insulator transition without a properly detailed consideration of long-range interactions.

We model the motion of vortices as coupled pancakes on neighboring, continuous planes separated by a distance z, with the applied magnetic field aligned perpendicularly to the planes. The off-lattice simulation models the motion of vortices referenced by a 2D coordinate $\mathbf{r}$ under the influence of pinning and repulsive

vortex interactions, and driving, line bending, and thermal forces:

$$m_l \ddot{\mathbf{r}}_i = -\eta_l \dot{\mathbf{r}}_i + \mathbf{f}_D + \mathbf{f}_T - \frac{\partial H(\{\mathbf{r}_1, \mathbf{r}_2 ...\})}{\partial \mathbf{r}_i}. \quad (1)$$

Here $f_D = \Phi_0 J/c$ is the Lorentz force per unit length due to an applied current density J perpendicular to the magnetic field. $\eta_l = (\Phi_0^2/2\pi\xi^2\rho_n c^2)$ is the Bardeen-Stephen viscous drag coefficient, with $\Phi_0 = (hc/2e)$ the flux quantum and ρ_n the normal state resistivity. The Langevin thermal force per unit length f_T is normalized to set the rms vortex velocity via the equipartition theorem. The Hamiltonian H is the sum of the line tension for bending, and vortex-vortex and vortex-disorder potentials per unit length constructed via London theory. The line tension is given by $\epsilon_l = \epsilon \ln(\kappa)\epsilon_0$ with $\epsilon = (m_c/m_{ab})^2$, $\kappa = \lambda/\xi$, $\epsilon_0 = (\Phi_0/4\pi\lambda)^2$, and λ magnetic penetration depth. The vortex interaction is given by a sum of pairwise interactions $V_{v-v}(\mathbf{r}) = \epsilon_0 K(\mathbf{r}/\lambda)$ with K a Hankel function [1], and the full long-range nature of the interaction is used. We model the correlated extended defects as smooth parabolic traps of width R_p and uniform depth $V_p = \epsilon_l/4$. Defects are randomly placed and aligned along the c axis.

In most cases the vortex mass per unit length m_l is overall quite small in comparison with the other parameters in Eq. (1) [18] and has thus usually been neglected in previous numerical studies in 3D of vortex dynamics [19]. However, in the case of superconductors near a Mott instability, such as the underdoped cuprates, the vortex mass can be enhanced as the system approaches a superconductor-insulator transition [20]. We thus keep m_l and simply relate it to the mass of the highly renormalized electrons confined to the vortex core region, $m_l = m_{\rm eff} n \pi \xi^2$, with n the electron density and $m_{\rm eff}$ the in-plane effective mass of the electron renormalized by strong interactions. While we have found that the vortex mass has an impact on the magnitude of the critical current, the relative J_c for different vortex densities do not drastically depend on the choices made.

Periodic boundary conditions are imposed in the planes to maintain constant global flux density, and open boundary conditions are employed along the c axis. Temperature is chosen which is high enough to allow individual vortices to be quickly accommodated to defects in the absence of a driving current but well below the glass temperature [4].

We measure all energies in units of the bare line bending energy ϵ_0 and measure all lengths in units of $d = 4\xi$. A natural time unit t_0 is chosen to be $\pi\kappa\eta_l d^2/\epsilon_l$ and the time step is further discretized in units of $0.01 t_0$ for the simulations. The current is measured in units of the BCS depairing current $J_0 = \Phi_0 c \kappa/12\sqrt{3}\pi^2\lambda^3$, and resistivity in terms of the Bardeen-Stephen flux-flow resistivity $\rho_{\rm BS} = B\Phi_0/(c^2\eta_l)$. The other parameters used in the simulations are dictated by values appropriate for $YBa_2Cu_3O_7$: $m_{\rm eff} = 5m_e$, $R_p = 2\xi$, $\xi = 17$ Å, $z = 12$ Å, $\kappa = 100$, and $\epsilon = 1/25$, giving $H_{c2} = 120$ T.

Our simulations were performed using up to 40 000 pancakes in a $128d \times 128d$ cell containing 80 planes, where finite size effects were found to be minimal. Measurements were taken over a $10^6 t_0$ interval after the system reached a steady state at roughly $3 \times 10^5 t_0$. We typically average the results over several hundred realizations of disorder particularly at smaller driving forces. We measure the average vortex velocity in the direction of the Lorentz force corresponding to the voltage drop across the sample, and determine the resistivity $\rho = \mathcal{E}/J$.

Our results for ρ as a function of J are shown for a series of vortex densities below and above the matching field B_Φ for two different values of B_Φ in Figs. 1(a) and 1(b). All error bars are equal to the symbol size. For the pinned Bose-glass regime $B < B_\Phi$ and for appreciable B_Φ [Fig. 1(a)], vortices are localized on separate columnar defects for small J until an abrupt transition to a moving regime ensues near $J \sim 0.1 J_0$ when the vortices simultaneously become unpinned. For larger driving currents, vortices are in the flux-flow regime and the resistivity approaches $\rho_{\rm BS}$. The depinning transition occurs within a narrow range of currents corresponding to single vortex pinning. Consequently, as B increases, the depinning transition occurs for smaller J and significantly broadens as the effective role of disorder diminishes relative to the vortex lattice interaction, in agreement with previous simulations [4]. The resistivity increases monotonically with increasing B as shown in the inset of Fig. 1(a). For values of B near and above the matching field, a low-current tail develops for small J and continues to increase as more and more interstitial vortices are not able to

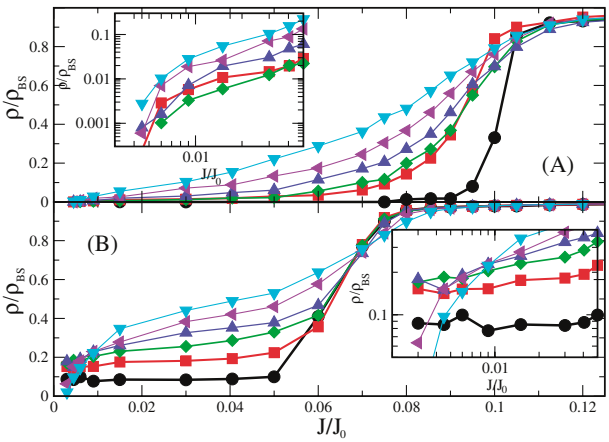

FIG. 1 (color online). Resistivity as a function of driving current for different values of the applied magnetic field referenced to the matching field B_Φ for $B_\Phi/H_{c2} \times 10^3 = 7.32$ (a) and 1.525 (b), respectively. The values of B/B_Φ are indicated as follows: Panel (a): 0.3 (circles), 0.8 (squares), 1 (diamonds), 1.25 (up triangles), 1.48 (left triangles), and 2 (down triangles); and Panel (b): 0.5 (circles), one (squares), 1.5 (diamonds), two (up triangles), three (left triangles), and four (down triangles). Solid lines are guides and become thicker for smaller fields. The insets show the low current resistivities.

reside on columnar defects due to the repulsion from the pinned vortices. These interstitial vortices are caged by the pinned vortices forming an weakly pinned interstitial glass with a much reduced critical current J_c, as suggested in Refs. [7,8]. As B is further increased, the interstitial glass melts into an interstitial liquid where channels of vortices flow around pinned vortices for arbitrarily small J and give a resistivity proportional to the fraction of interstitial to pinned vortices. We note that for our parameter choices we do not observe a Mott insulating phase as we always have interstitial vortices for $B/B_\Phi = 1$ due to the long-range vortex repulsion and high temperatures.

Important differences, however, are observed for smaller values of B_Φ [Fig. 1(b)]. For $B < B_\Phi$ in this case, the transition to depinning occurs at lower J and is substantially broadened compared to Fig. 1(a). A nonmonotonic dependence of the resistivity appears as shown in the inset of Fig. 1(b). For small J, ρ rises with increasing B for $B/B_\Phi < 1.5$ and becomes greater than $0.1\rho_{BS}$ for $B \sim B_\Phi$ as the interstitial glass melts into an interstitial liquid. However, at larger fields ρ decreases and becomes less than $0.1\rho_{BS}$ for fields near 3 times the matching field. This indicates that for low B_Φ the Bose glass melts into an interstitial liquid near the matching field and recrystallizes into an interstitial glass at larger values of B/B_Φ, in contradiction to the phase diagram proposed previously [7].

We can make this more quantitative by defining a critical current density J_c as the value of J corresponding to $\rho = 0.1\rho_{BS}$. Values for J_c as a function of B/B_Φ obtained for MD runs of different B_Φ are shown in Fig. 2. Here we have normalized J_c to the maximal values J_c^{max} determined for small B/B_Φ. For large B_Φ, J_c/J_c^{max} decreases monotonically with B/B_Φ with a gradual falloff near the matching field. For smaller values of B_Φ this falloff becomes much more abrupt, suggesting that strength of the kink in the melting curve would be dependent on the value of B_Φ, reconciling previous experiments [5,6,9–15]. For even smaller B_Φ, the falloff is dramatic and the interstitial glass weakens appreciably and melts ($J_c = 0$) near a critical value of $B_\Phi^c/H_{c2} \sim 1.9 \times 10^{-3}$. Remarkably, the critical current resurrects for larger values of the magnetic field and has a broad peak near $B = 3B_\Phi$ for $B_\Phi/H_{c2} \times 10^3 = 1.906$ before falling off again at still larger fields, as observed in $Tl_2Ba_2CuO_{6+\delta}$ [6]. However, we see that still smaller values of B_Φ yield critical current peaks at larger values of B/B_Φ. While we expect that the actual value of the critical field B_ϕ^c might depend on our choice of defining J_c, we do not expect the re-entrance into the interstitial glass to be qualitatively changed. A proposed phase diagram which encompasses our results for different B_Φ is given in Fig. 3.

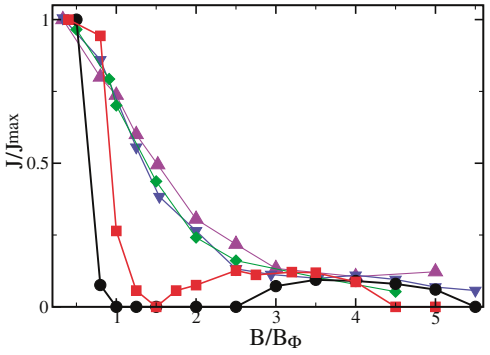

FIG. 2 (color online). Normalized critical currents as a function of B/B_Φ for different densities of columnar defects. The density of defects is given by $10^3 \times B_\Phi/H_{c2} = 1.525, 1.906, 3.05, 4.88,$ and 7.32 for circles, squares, down triangles, diamonds, and up triangles, respectively. Guide lines are thicker for smaller fields.

Using renormalization group arguments it was shown by Nelson and Seung that for clean systems the interactions between vortex lines are renormalized to zero near H_{c1} and leads to the melting of the Abrikosov lattice as $H \to H_{c1}$ [17]. Thus we might expect that the melting of the interstitial glass for $B - B_\Phi \geq 0^+$ is similar to the melting of the vortex lattice near H_{c1} [2,17]. However, there are distinct differences for B less than or greater than B_ϕ. For $B < B_\Phi$ vortex localization onto unoccupied columnar defects helps to reduce vortex fluctuations and one might expect the Bose glass to be stable near H_{c1} as vortices occupy the strongest defects. Yet once $B > B_\Phi$ the interstitial vortices feel a much reduced and screened defect interaction and suffer the downward renormalization of the shear modulus as in clean systems. This is

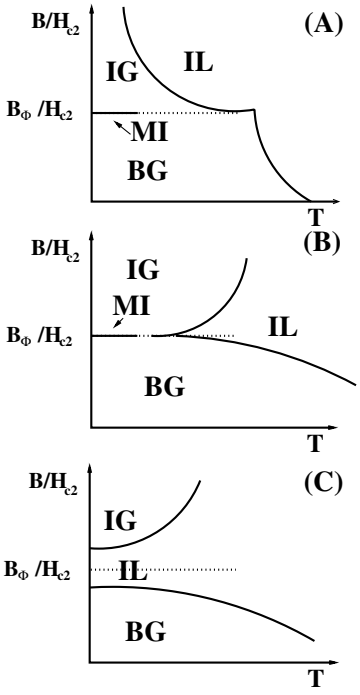

FIG. 3. Conjectured phase diagram for large (a), intermediate (b), and small (c) matching field densities.

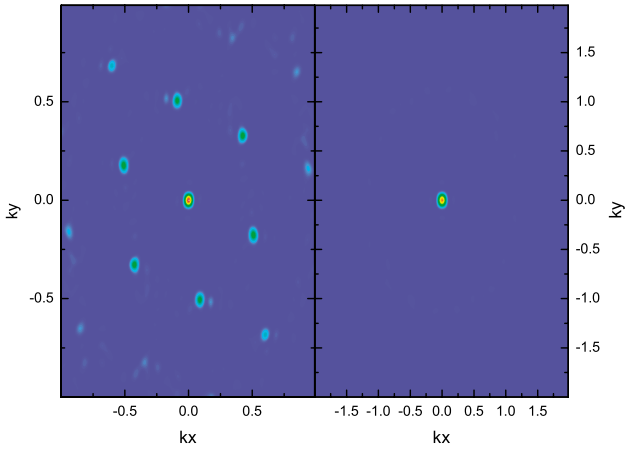

FIG. 4 (color online). Structure factor in the pinned phase at 3 times the matching field $B/B_\Phi = 3$ for $10^3 \times B_\Phi/H_{c2} = 1.525$ (left) and 7.32 (right) panels, respectively. Momentum is measured in units of $1/d$.

borne out in our simulations for small defect concentrations as measured by B_ϕ/H_{c2}. As the field increases our simulations indicate that the interstitial glass recrystallizes. This can be viewed as a hardening of the shear modulus for increasing fields as the role of interactions increases.

What leads to the recrystallization of the melted interstitials at larger values of B for small defect concentrations? At large vortex concentrations the Coulomb potential is effectively short range due to screening and the effects of disorder are also screened by flux line collisions, and indeed our results are consistent with prior simulations for contact repulsive potentials [4]. The system favors forming dislocations at larger fields and vortex domains are easily depinned. For smaller vortex concentrations, new physics arises as screening is no longer effective and the bare long-range repulsive forces encourage longer-range ordering concomitant with decreased prevalence of dislocations and subsequent enhanced vortex pinning.

To check these ideas, we plot in Fig. 4 time-averaged structure plots for $B = 3B_\Phi$ at two values of B_Φ. While long-range order is not seen even on the length scale of our simulations, it is clear that orientational short-range order is more prevalent for smaller B_Φ, with subsidiary structure peaks at the reciprocal lattice vectors up to $1/2$ the height of the central ($Q = 0$) peak. We would expect that for still smaller values of B_Φ positional order would grow for systems of fixed finite size L with the possible formation of Bragg-like peaks.

In summary, we have presented numerical simulations of interacting vortex dynamics in the presence of columnar disorder as a function of B/B_Φ and B_Φ/H_{c2}. We find a monotonic decrease in the critical current for large values of B_Φ, with a sharp dropoff near the matching field, consistent with prior notions of the weakly pinned interstitial glass emerging at higher fields. For smaller values of B_Φ however, we see abrupt melting at $B = B_\Phi$ and recrystallization near $B = 3B_\Phi$ of the interstitial glass, suggesting modifications to the phase diagram due to the role of long-range interactions even for columnar disorder. As the interacting vortex problem with columnar disorder in 3D can be mapped onto world lines of interacting disordered bosons in 2D, the intervening melted phase observed here for small B_Φ may be related to the intervening phase observed both in the Bose glass in the presence of a transverse field [15] and the intervening dissipative metallic phase observed in 2D MoGe films [21].

T. P. D. would like to thank M. J. P. Gingras and T. F. Rosenbaum for many useful discussions. T. P. D. would like to acknowledge support from NSERC, PREA, and the Alexander von Humboldt Foundation.

[1] G. Blatter *et al.*, Rev. Mod. Phys. **66**, 1125 (1994).
[2] D. Nelson, Phys. Rev. Lett. **60**, 1973 (1988); D. Nelson and V. M. Vinokur, Phys. Rev. Lett. **68**, 2398 (1992); Phys. Rev. B **48**, 13060 (1993).
[3] R. T. Scalettar *et al.*, Phys. Rev. Lett. **66**, 3144 (1991); N. Trivedi *et al.*, *ibid.* **67**, 2307 (1991); W. Krauth and N. Trivedi, Europhys. Lett. **14**, 627 (1991); K. Bernardet *et al.*, Phys. Rev. B **65**, 104519 (2002); P. Sen *et al.*, Phys. Rev. Lett. **86**, 4092 (2001).
[4] A. Nandgaonkar *et al.*, Phys. Rev. B **66**, 104527 (2002).
[5] K. M. Beauchamp *et al.*, Phys. Rev. Lett. **75**, 3942 (1995).
[6] E. R. Nowak *et al.*, Phys. Rev. B **54**, 12 725 (1996).
[7] L. Radzihovsky, Phys. Rev. Lett. **74**, 4923 (1995).
[8] A. I. Larkin and V. M. Vinokur, Phys. Rev. Lett. **75**, 4666 (1995).
[9] T. K. Worthington *et al.*, Phys. Rev. B **46**, 11 854 (1992).
[10] L. Krusin-Elbaum *et al.*, Phys. Rev. Lett. **72**, 1914 (1994).
[11] G. Nakielski *et al.*, Phys. Rev. Lett. **76**, 2567 (1996).
[12] A. V. Samoilov *et al.* Phys. Rev. Lett. **76**, 2798 (1996).
[13] A. Mazilu *et al.*, Phys. Rev. B **58**, 8909 (1998).
[14] A. W. Smith *et al.*, Phys. Rev. B **59**, 11 665 (1999).
[15] A. W. Smith *et al.*, Phys. Rev. Lett. **84**, 4974 (2000); Phys. Rev. B **63**, 64514 (2001).
[16] A. L. Fetter, P. C. Hohenberg, and P. Pincus, Phys. Rev. **147**, 140 (1966).
[17] D. R. Nelson and S. Seung, Phys. Rev. B **39**, 9153 (1989).
[18] H. Suhl, Phys. Rev. Lett. **14**, 226 (1965); G. Baym and E. Chandler, J. Low Temp. Phys. **50**, 57 (1983); M. W. Coffey and J. R. Clem, Phys. Rev. B **44**, 6903 (1991); D. M. Gaitonde and T. V. Ramakrishnan, Phys. Rev. B **56**, 11 951 (1997); E. B. Sonin *et al.*, Phys. Rev. B **57**, 575 (1998); G. E. Volovik, JETP Lett. **67**, 528 (1998); N. B. Kopnin and V. M. Vinokur, Phys. Rev. Lett. **81**, 3952 (1998).
[19] A. van Otterlo *et al.*, Phys. Rev. Lett. **81**, 1497 (1998); C. Olson *et al.*, Phys. Rev. Lett. **85**, 5416 (2000).
[20] S. Doniach and M. Inui, Phys. Rev. B **41**, 6668 (1990); M. V. Pedyash *et al.*, IEEE Trans. Appl. Supercond. **5**, 1387 (1995).
[21] A. Yazdani *et al.*, Phys. Rev. Lett. **74**, 3037 (1995); D. Ephron *et al.*, Phys. Rev. Lett. **76**, 1529 (1996).